CRYPTIC MICROBES IN ANTARCTICA: DETERMINING THE LIMITS OF BIOTIC DETECTION VIA SATELLITE IMAGERY

Sarah N. Power[1], Mark R. Salvatore[2], and J. E. Barrett[1]

[1]Department of Biological Sciences, Virginia Polytechnic Institute and State University
[2]Department of Astronomy and Planetary Science, Northern Arizona University

Abstract

Autotrophic microbial communities (*e.g.*, cyanobacteria, moss) are the primary drivers of carbon cycling in the McMurdo Dry Valleys, Antarctica. Dense microbial mats occupy aquatic areas, while surface soil biocrusts occur at much lower densities across the soil landscape. Our previous research shows that NDVI approaches with multispectral satellite data are successful at quantifying the abundance of surface microbial communities in high-density areas along aquatic margins. Given the broader spatial extent of the arid landscape outside of the aquatic margins, we predict a significant proportion of the valley-wide ecosystem carbon budget is represented by patchily distributed biocrust. Here, we describe recent remote sensing and field-based survey and sampling approaches to measure biocrust distribution in "dry" soil environments. We found that spectral parameters like NDVI applied to WorldView-2 (WV-2) satellite imagery can be influenced by lithological surface composition. Therefore, we implemented additional multispectral and hyperspectral tools to quantify the detectability of biocrust in this region. Using a principal components analysis, we have currently determined a detection threshold of ~ 20 mg/cm^2 ash-free dry mass of active biocrust. Additionally, we applied linear spectral unmixing models to WV-2 data using lab-derived spectra of biotic and abiotic materials. This work is part of ongoing efforts to refine the carbon budget for this region and to examine controls over the distribution and activity of these critical soil communities.

Introduction

Autotrophic microbial communities are the drivers of carbon cycling in the McMurdo Dry Valleys (MDV) of Antarctica. These microbial communities consist of cyanobacteria, green algae, diatoms, and moss, are home to microscopic invertebrates, and can form mm – cm thick mats within and nearby aquatic areas and also thin terrestrial crusts on the soil surface. Dense microbial mats commonly inhabit aquatic areas in the Taylor Valley, Antarctica while the majority of the landscape is terrestrial where biological surface crusts (*i.e.*, biocrusts) can occupy with much lower densities. The terrestrial landscape of this region is spatially extensive, and although biocrusts on the soils are sparser than the aquatic microbial mats, we anticipate the terrestrial MDV soils contain a significant amount of carbon cumulatively. Assessing the detectability of biocrusts is a critical first step in ultimately estimating terrestrial carbon stocks in this region. In this report we present the first assessment of biocrust detectability in the MDV terrestrial landscape using WorldView-2 and -3 multispectral satellite imagery, laboratory hyperspectral spectroscopy, and *in-situ* soil and biological ground truthing.

The McMurdo Dry Valleys are the largest contiguous ice-free area on the Antarctic continent, with approximately 4500 km^2 of exposed soil, stream, and lake ecosystems (Levy 2013). Glacial meltwater during the austral summer (*i.e.*, 24 hours daylight) forms streams that flow for up to 10 weeks per year (McKnight et al. 1999). These streams feed into perennially ice-covered lakes along the floor of Taylor Valley. While dense microbial mats occupy streams and lake margins (Fig. 1a), biocrusts occupy terrestrial areas in relatively wet depressions, beside snowpacks, and even drier soils (Fig. 1b, c). The microbial mats and biocrusts are dominated by cyanobacteria (*Nostoc*, *Oscillatoria*, and *Phormidium*) and also contain chlorophyta (green algae), various diatom species (bacillariophyta) (Alger et al. 1997), and mosses (*Bryum* and *Hennediella*) (Schwarz et al. 1992; Pannewitz et al. 2003). In addition, simple metazoan communities of nematodes, rotifers, and tardigrades inhabit the soils and sediments of this region (Freckman and Virginia 1997). Nematodes (*i.e.*, microscopic roundworms that consume cyanobacteria and other microbes) are the most widely distributed metazoan taxa in this region (Freckman and Virginia 1997). Though, given such low soil biomass, negligible grazing influences on microbial mat communities (Treonis et al. 1999) makes the MDV a simple system for studying biocrusts.

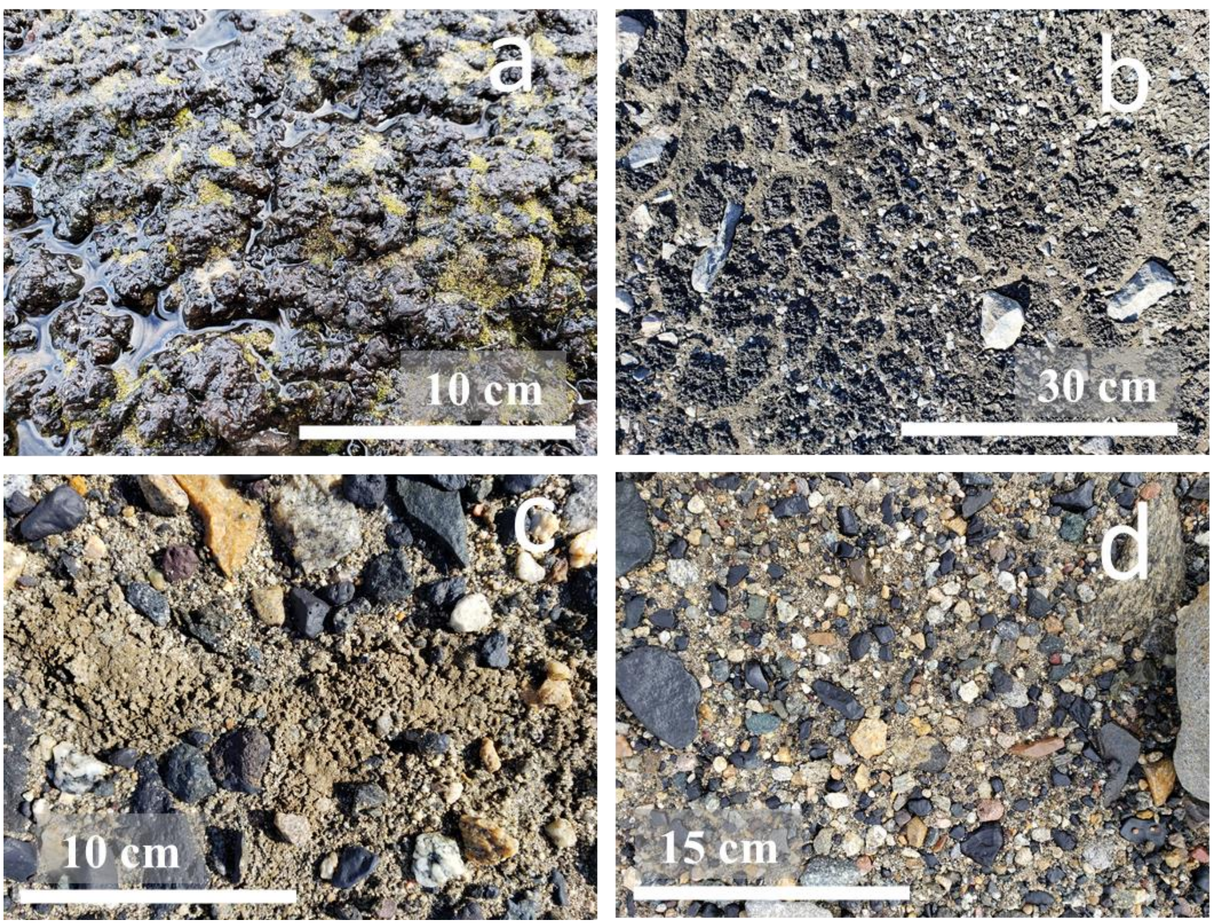

Fig. 1 Photos of (**a**) dense, wet microbial mat in the Canada Flush (see Power et al. 2020); (**b**) dense biocrust downhill from snowpack (Plot 09); (**c**) sparse, incipient biocrust in moist depression (Plot 26); and (**d**) representative low productivity desert pavement (Plot 31).

Taylor Valley is composed of tills (*i.e.*, unsorted soil/rock material deposited directly from glacial ice) from different sequences of glaciations. Most notably, the Ross till (Fig. 2), deposited directly from Ross Sea ice sheets in the late Pleistocene (Bockheim et al. 2008), is on the eastern side of Taylor Valley and is considered the most productive area of this valley, as it is closest to the coast, is relatively humid, has relatively high soil moisture content compared to the other climate zones in this region (Marchant and Denton 1996; Doran et al. 2002), and has the most active and fully functioning soil communities (Adams et al. 2006; Barrett et al. 2006b). While soil environments outside of stream channels do not commonly support visible microbial mat biomass, they are, however, spatially extensive compared to the wetted areas. Due to the broad spatial extent of these terrestrial environments, even sparse spatial distributions of biocrusts could sum to more biomass overall. Our fundamental motivation for this study is relevant for understanding carbon budgets, predicting future carbon stocks, and for generally understanding the basic ecology of this ecosystem. To quantify the detectability of biocrusts throughout the MDV terrestrial landscape, systematic and scalable techniques are required.

Our previous research has shown the utility of multispectral satellites WorldView-2 and WorldView-3 (WV-2/3) in detecting microbial mats in densely colonized areas near streams on the Ross till using the Normalized Difference Vegetation Index (NDVI) and other reflectance parameters (Salvatore 2015; Salvatore et al. 2020; Power et al. 2020) and also spectral unmixing methods using *in-situ* hyperspectral measurements (Salvatore et al. 2021). NDVI evaluates the relationship between reflectance at 680 and 800 nm where photosynthetic materials exhibit a strong diagnostic signal. This signal is caused by vegetation, which has a unique spectral signature of absorbance in the visible wavelengths (due to the activity of chlorophyll-a and other pigments) and strong reflectance in near-infrared regions due to scattering and reflectance by cell walls. Additionally, we have observed NDVI values indicative of photosynthetic activity in upland areas not connected to streams or lakes (Power et al. 2020). While NDVI is a useful indicator of biological activity in relatively dense areas near streams, previous efforts originally derived for high-productivity areas were broadly applied to the entirety of the terrestrial landscape (Salvatore et al. 2021), though the accuracy of this application was not fully explored at the time. It was unknown whether these anomalously high NDVI terrestrial areas do indeed support photosynthetic activity, or if they were simply influenced by background noise of the orbital data or were associated with some other lithological or topographical attribute.

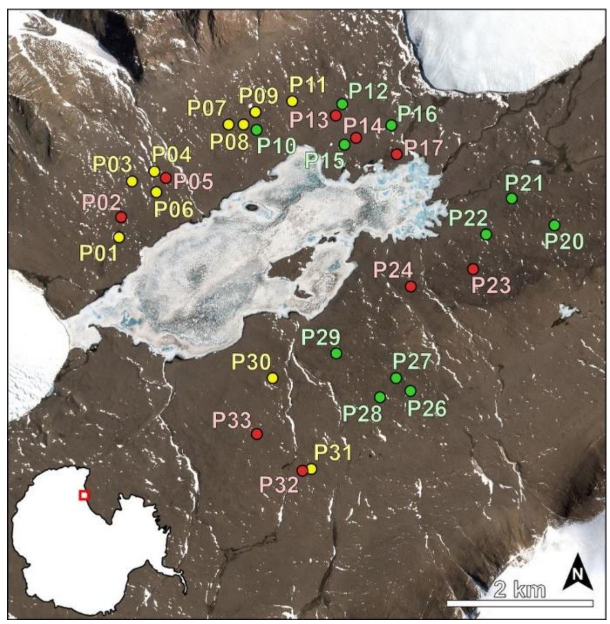

Fig. 2 True color image of Ross till region with the 30 sampling locations identified with varying NDVI values (green refers to “high” NDVI, yellow “variable”, and red “low”) based upon preliminary data that were used to select a range of sites. Inset in bottom left corner shows Antarctica with red box outlining the McMurdo Dry Valleys. Imagery © 2018 DigitalGlobe, Inc.

These terrestrial environments have received significant attention and have been shown to support fully functioning and active food webs, even given the low diversity of taxa in soils (Freckman and Virginia 1997; Courtright et al. 2001; Barrett et al. 2006a; Barrett et al. 2006b; Poage et al. 2008). The MDV soil community consists of cyanobacteria (and other prokaryotes), algae (*e.g.*, diatoms), mosses, lichens, nematodes, tardigrades, rotifers, fungi, protozoans (*i.e.*, flagellates, amoebae, ciliates), and microarthropods (*i.e.*, springtails and mites) (Adams et al. 2006). Because these soils host active microbial and invertebrate communities and have detectable surface chlorophyll-a content (*e.g.*, Barrett et al. 2004), we predicted these "NDVI anomalies" scattered throughout the terrestrial environment are suggestive of photosynthetic life supporting active food webs. While the wetter soils (*e.g.*, stream and lake margins) receive more research attention, we believe the terrestrial soils may be equally important, if not more, to the overall carbon budget of the MDV. Therefore, to ultimately refine the carbon budget for this region and to examine controls over the distribution and activity of these critical soil communities, we must first determine the detectability of biocrusts in this region. Combining multispectral satellite data, laboratory hyperspectral measurements, and biological ground truthing, we test the detectability of cryptic patches of biological activity in the form of biocrusts in terrestrial soils of the McMurdo Dry Valleys.

Methods

Field collection

Using December 2018 WV-2 imagery, we identified 30 locations on the Ross till with varying NDVI values. These terrestrial sites consist of relatively dry soils unconnected by stream or lake margins (*i.e.*, referred to as "upland areas"). In late December 2019, we located and sampled these 30 varying NDVI sites. We obtained photographs and noted the field conditions (*e.g.*, dry soils with no indication of biological activity, wet soils with snowpack nearby, area dominated by specific geology, *etc*.). We collected a top layer of soil and rock from all sites for subsequent hyperspectral analysis. At 12 of the sites, we established 5 m x 5 m plots and collected 5 top layer soil samples (one from each corner and center) of a known area (128 cm^2) for pigment analysis (chlorophyll-a, scytonemin, and carotenoids) and ash-free dry mass (AFDM) for organic matter content. We also collected underlying soil (top 10 cm) for gravimetric water content (GWC), electrical conductivity (EC), pH, inorganic nitrogen (N) concentration in the form of ammonium (NH_4^+) and nitrate (NO_3^-), inorganic phosphorus (PO_4^{3-}) concentration, total organic carbon (TOC), total nitrogen (TN), and invertebrate abundance (nematodes, tardigrades, rotifers).

Laboratory analyses

Using the surface layer soil samples, we determined pigment concentration using a trichromatic spectrophotometric method for chlorophyll-a, carotenoids, and scytonemin at 663, 490, and 384 nm, respectively (Garcia-Pichel and Castenholz 1991). Throughout the process, care was taken to avoid exposing the samples to light, as chlorophyll-a degrades with light exposure. The samples were first dried at 105°C for 24 hr, sieved through a 4 mm sieve, and extracted for 24 hr at ambient temperature in 90% unbuffered acetone using a 3.75:10 soil to solvent ratio, based on protocols from Couradeau et al. (2016) and MCM LTER standard methods. After centrifugation, the extracts were analyzed on a spectrophotometer using 10 mL cuvettes. The absorbances contributed by each pigment were calculated using the trichromatic equations outlined in Garcia-Pichel and Castenholz (1991), and the pigment concentrations were calculated using the Beer-Lambert Law with the extinction coefficients of 89.7 L g^{-1} cm^{-1} for chlorophyll-a (Couradeau et al. 2016), 112.6 L g^{-1} cm^{-1} for scytonemin (Brenowitz and Castenholz 1997), and 262 L g^{-1} cm^{-1} for carotenoids (Thrane et al. 2015). Additionally, the top layer soil samples were measured for AFDM by weighing a known area of sample, combusting at 550°C for 24 hr using a muffle furnace, gently stirring samples halfway through combustion, and reweighing after cooling in a desiccator. Given the extremely low clay content of soils in this region (Barrett et al. 2006a), the rehydration of clays was assumed negligible, so we did not rewet samples.

Using the underlying soil samples, we measured gravimetric water content, and pH and electrical conductivity using a 1:2 and 1:5 soil to DI H_2O slurry, respectively. We also extracted inorganic N in the form of NH_4^+ and NO_3^- with a 2:5 soil to potassium chloride extract, and we extracted inorganic P in the form of PO_4^{3-} with a 1:5 soil to sodium bicarbonate extract using a Lachat flow injection analyzer. Additionally, we measured TOC and TN using an Elementar vario cube TOC/TN analyzer. Invertebrate abundance was enumerated on the underlying soil using a modified sugar-centrifugation method (Freckman and Virginia 1993).

Spectral collection and analysis

WorldView-2 (DigitalGlobe, Inc.) is an 8-band multispectral satellite on polar orbit with 1.84 m resolution at nadir. Images acquired between December 2018 and December 2019 were used to identify varying NDVI upland terrestrial areas and correlate them to biological ground truthing data, respectively. The imagery was georeferenced using ground control points and then obtained from the University of Minnesota's Polar Geospatial Center (PGC) through a cooperative agreement between the NSF and National Geospatial-Intelligence Agency (NGA). Data were subsequently processed to atmospherically corrected surface reflectance using five spectral ground validation targets acquired in the field during the 2018-2019 austral summer (Salvatore et al. 2021). Band-specific linear relationships between top-of-atmosphere reflectance data and ground validation spectra were applied to the entirety of the satellite images to remove atmospheric contributions to the observed signal. The NDVI parameter was calculated using the Environment for Visualizing Images (ENVI, Harris Geospatial) software package. NDVI is a common vegetation index used for assessing whether pixels contain photosynthesizing surface materials (Tucker 1979). NDVI was calculated using the spectral reflectance measurements acquired in the near-infrared (WorldView-2 Band 7, centered at 831 nm) and red (WorldView-2 Band 5, centered at 659 nm) regions. The varying NDVI locations were identified as occurring within depressions, on slopes or hills, and within rocky outcrops by using a (DEM) of 1 m resolution (Fountain et al. 2017). NDVI was extracted from the 4 pixels centered at each plot location, based on GPS coordinates taken during sampling and visually confirming plot location via nearby boulders, snowpacks, etc. The primary WorldView-2 image used in this analysis (103001009FA0AE00) was acquired on December 3, 2019, approximately three weeks before our field sampling campaign. Map products were created using ArcMap (ESRI).

In addition to NDVI, we also calculated the Simple Ratio Index (SR), the Red-Edge Simple Ratio Index (SRre), and the Normalized Pigment Chlorophyll Index (NPCI). SR and NPCI have been shown effective in detecting dry biocrust from the Colorado Plateau with a portable spectroradiometer (Young and Reed 2017). SR was calculated using the NIR and Red bands, SRre was calculated using the NIR and Red-Edge bands, and NPCI was calculated using the Red and Coastal bands. Each of the parameter values were extracted from the pixels within each plot and averaged to estimate an average NDVI, SR, SRre, and NPCI value for each of the 12 plots. The same was performed using the average reflectance values for each of the WV-2 8 bands per plot as well.

As part of a laboratory study, we created mixtures of sample biocrust and Ross till soil of varying percent (0 - 100%) biocrust by weight (g/g). To estimate detection limits of biocrust, we collected hyperspectral measurements of the biocrust and soil mixtures in the laboratory. These data were acquired using an Analytical Spectral Devices (ASD) FieldSpec4 high-resolution hyperspectral reflectance spectrometer, set up for use in a stable lab environment. Data were collected between 350 and 2500 nm with 1 nm sampling. Halogen lamps were used to illuminate the samples at 30° off-nadir, while reflectance was measured using the ASD's fiber optic cable at nadir. Measurements represent an average of 50 individual spectra, which were averaged to minimize noise and to ensure a representative spectral signature. Hyperspectral measurements of pure soil and biocrust samples were downsampled to WorldView-2 resolution, and we applied spectral linear unmixing models to the remaining mixtures. We then compared how well the modeled biocrust abundances correlated to the known biocrust abundances that we tested. Hyperspectral reflectance data were also acquired in the laboratory for surface layer soil samples collected in the field. These surface soil samples were shipped frozen from Virginia Tech to Northern Arizona University where the spectral measurements were acquired.

Statistical analysis

Statistical analyses were performed using R Statistical Software version 4.0.3 (R Core Team). Principal components analyses (PCA) on correlation and covariance were executed using R to visually compare plots in terms of their soil habitat environment and orbital reflectance spectra with vegetation indices, respectively. Additionally, a correlation analysis was performed on the laboratory spectral data comparing the actual biocrust abundance to the modeled biocrust abundance.

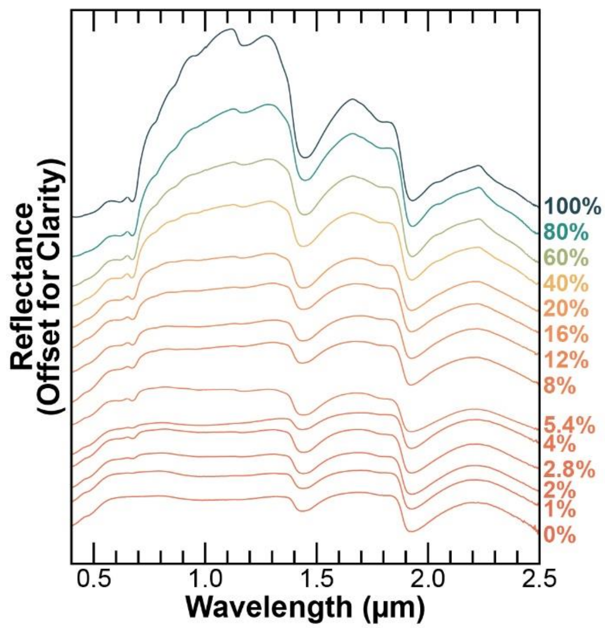

Fig. 3 Hyperspectral signatures of laboratory mixtures of soil and biocrust at varying percentages of biocrust displayed on the right. Chlorophyll absorption feature clearly identifiable at ~ 0.68 μm.

Results

From the hyperspectral measurements of the soil and biocrust sample mixtures in the laboratory, there was a chlorophyll absorption feature visible at ~ 680 nm for all mixtures containing biocrust (Fig. 3), including the lowest abundance sample of 1% biocrust by weight (g/g). Using the pure (100%) soil and biocrust samples, we downsampled the hyperspectral data to WorldView-2 resolution and applied spectral linear unmixing models. We obtained modeled biocrust abundance for all mixtures, and when compared to the actual measured biocrust abundance, there was a near-perfect fit between the modeled and measured biocrust abundance with an R^2 of 0.99 (Fig. 4).

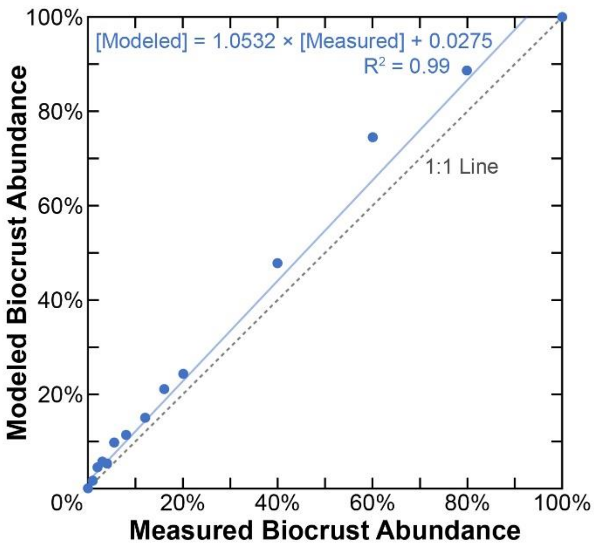

Fig. 4 Highly significant fit (R^2 = 0.99) between modeled (spectral linear unmixing) and measured biocrust abundance using laboratory mixtures of soil and biocrust.

After locating the varying NDVI sites in the field, we determined that many of the locations appeared as suitable habitats (*i.e.*, wet soils, depressions, snowpacks nearby, *etc*.). There was one location in particular with dense biocrust present (Plot 09), while other plots were identified as possibly containing sparse biocrust cover or representative low productivity desert pavement. Alternatively, there were several plot locations that were originally categorized as having relatively high NDVI from orbital data that upon examination, were dry, barren, and seemingly uninhabitable. Many of these relatively high NDVI locations, however, were scattered with bright orange rocks visually identified as oxidized granite (Fig. 5). While many of these relatively high NDVI locations seemed indicative of biological activity, there were clearly some locations where geological surface materials were driving NDVI rather than biology. Additionally, using the hyperspectral measurements collected from the field plot samples, there are clear spectral differences between the plots, for example, Plots 09 (biocrust) and 20 (oxidized granite). While they both have relatively high NDVI, it is evident that the shape of their spectral signatures is very different. These differences are further illustrated in Figure 6, which compares the spectral shape of relatively high NDVI Plots 09 and 20 with a barren soil Plot 02.

Fig. 5 Photos of relatively high NDVI Plot 20 oxidized granite (**a**) and close-up granite view (**b**).

Table 1. Biological variables averaged (n=5) within each of the intensively sampled plots.

Plot ID	AFDM (mg cm^{-2})	Chlorophyll (μg cm^{-2})	Carotenoid (μg cm^{-2})	Scytonemin (μg cm^{-2})	Nematodes (# kg^{-1} dry soil)	Rotifers (# kg^{-1} dry soil)	Tardigrades (# kg^{-1} dry soil)
P01	5.35	0.009	0.062	0.864	362	0	2
P09	28.29	4.974	2.141	77.395	1102	30	1822
P10	2.12	0.007	0.031	0.331	1453	32	2
P14	4.06	0.006	0.063	0.800	959	0	0
P17	3.90	0.005	0.040	0.683	449	0	0
P22	2.19	0.005	0.027	0.285	0	0	0
P23	2.99	0.002	0.040	0.399	85	0	0
P27	3.18	0.006	0.032	0.432	168	0	0
P28	2.55	0.003	0.033	0.379	495	2	0
P30	3.46	0.005	0.036	0.272	0	0	0
P31	3.87	0.007	0.037	0.309	0	0	0
P33	2.61	0.004	0.019	0.137	875	0	0

Table 2. Physical and chemical variables averaged (n=5) within each of the intensively sampled plots where "GWC" refers to gravimetric water content, "TOC" total organic carbon, and "TN" total nitrogen.

Plot ID	GWC (g/g)	Electrical Conductivity (μS cm^{-1})	pH	μg NH_4^+ g^{-1} dry soil	μg NO_3^- g^{-1} dry soil	μg PO_4^{3-} g^{-1} dry soil	mg TOC g^{-1} dry soil	mg TN g^{-1} dry soil
P01	0.06	2330	8.4	0.12	57.87	3.56	1.00	0.133
P09	0.06	70	8.5	0.09	0.86	3.12	2.08	0.215
P10	0.02	112	9.9	0.02	0.00	4.47	2.56	0.108
P14	0.06	2311	8.6	0	48.30	12.19	1.95	0.258
P17	0.02	1095	8.8	0	65.79	5.85	1.17	0.165
P22	0.05	2152	9.5	0.02	65.51	18.65	5.01	0.217
P23	0.02	907	9.6	0	13.43	3.34	0.94	0.096
P27	0.03	656	8.4	0	4.32	2.71	2.22	0.121
P28	0.08	515	8.9	0	5.17	3.00	2.17	0.129
P30	0.04	2347	9.0	0	33.40	3.70	2.18	0.131
P31	0.05	2431	8.2	0.01	27.68	1.70	1.55	0.115
P33	0.02	130	9.6	0.03	0.12	2.30	1.53	0.102

There was inter-plot variation among the sites in terms of biological variables (concentration of chlorophyll-a, carotenoids, scytonemin, AFDM, and population of invertebrates) (Table 1) and physical and chemical variables (gravimetric water content, electrical conductivity, pH, NH_4^+, NO_3^-, PO_4^{3-}, TOC, and TN concentration) (Table 2). Notably, Plot 09 with visible biocrust had the highest diversity consisting of all three nematode species (*Scottnema*, *Eudorylaimus*, and *Plectus*), tardigrades, rotifers, and even ciliates. While *Scottnema* was present in relatively high abundances throughout the plots, there were several plots without any invertebrates present (P22, 30, 31). The majority of samples had NH_4^+ concentration below detection, except for Plots 01, 09, 10, 22, 31, 33, which were detectable, though very low concentrations.

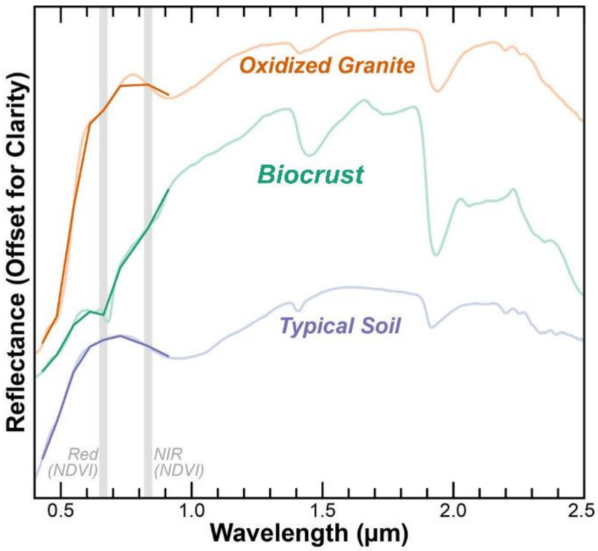

Fig. 6 Three spectral signatures illustrating relatively high NDVI from biocrust (Plot 09) and oxidized granite (Plot 20), and low NDVI from typical soil (Plot 02). Spectra downsampled to WV-2 resolution are shown in bold. Gray bars outline the region of NDVI calculation.

In a principal components analysis on correlation using the physical and chemical variables from the field samples, the plots vary in ordination space based on gravimetric moisture content, pH, electrical conductivity, and inorganic N and P content (Fig. 7). Most notably, in a principal components analysis on covariance using the WV-2 band reflectance (B1 – B8) and vegetation indices (NDVI, NPCI, SR, SRre), there is separation in ordination space between the predominantly oxidized granite, biocrust, and bare soil plots (Fig. 8). There is a visual gradient of plots moving from bare soil to dense biocrust in the ordination space, with the oxidized granite plots more spectrally dissimilar away from this gradient.

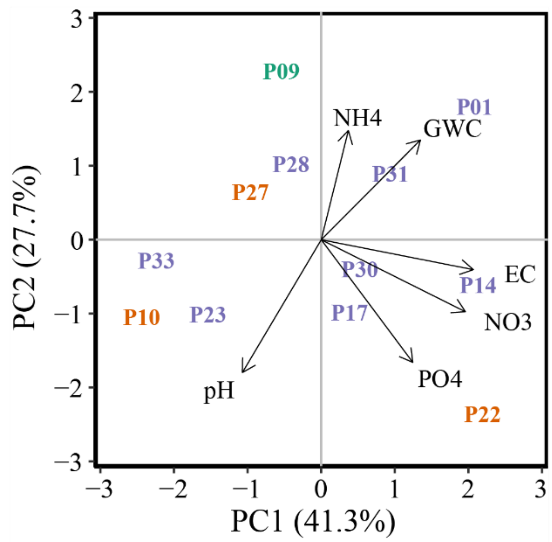

Fig. 7 Principal components analysis ordination on correlation of the 12 intensively sampled plots. Color distinction follows that of Fig. 6 (plots with ground cover consisting mainly of oxidized granite are shown in orange, biocrust in green, and typical soil in purple). Vectors represent correlations of soil habitat variables with PCA ordination axes (all displayed correlations are significant, $p < 0.05$).

Discussion

Under ideal conditions in a laboratory, we determined that biocrust in soil mixtures is successfully detectable at abundances down to just 1% biocrust by weight (g/g) using hyperspectral reflectance measurements. Even at such low abundances, the chlorophyll absorption feature at ~ 680 nm is visible from this high-resolution dataset (Fig. 3). Using the soil and biocrust mixtures ranging from 0% to 100% biocrust by weight, we applied spectral linear unmixing models to the reflectance spectra using the pure (100%) soil and biocrust endmembers. The data were first downsampled from hyperspectral resolution to WorldView-2 multispectral resolution to more accurately compare with the resolution of the orbital data we later used. Comparing the modeled biocrust abundance of each sample mixture to the actual measured biocrust abundance, there was a near-perfect fit between the modeled and measured abundance with an R^2 of 0.99 (Fig.

4). This demonstrates successful laboratory detection of varying biocrust abundances using spectral linear unmixing methods. This offers promise for translating this method to orbital data, knowing the field data brings added complexity in comparison to these ideal laboratory mixtures. These added complexities include varying surface composition and moisture, coarser resolution reflectance spectra, and atmospheric contributions.

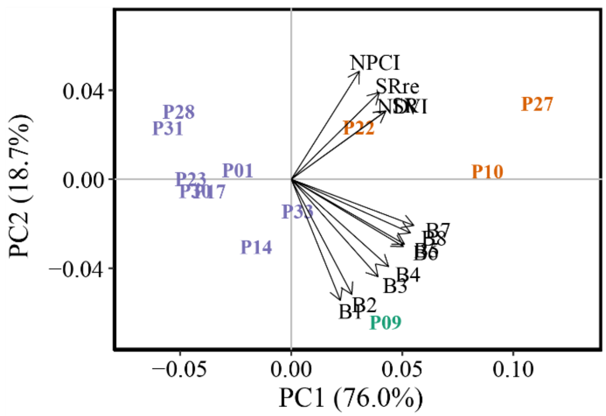

Fig. 8 Principal components analysis ordination on covariance of the 12 intensively sampled plots. Color distinction follows that of Fig. 6 (plots with ground cover consisting mainly of oxidized granite are shown in orange, biocrust in green, and typical soil in purple). Vectors represent correlations of WorldView-2 band reflectance (B1 - B8) and vegetation indices (NDVI, NPCI, SR, SRre) with PCA ordination axes (all displayed correlations are significant, $p < 0.05$).

Surface composition of the MDV environment is highly complex, and it was evident during our ground truthing campaign that geology would be a strong factor in testing the utility of orbital data for the detection of low density biocrusts. Several plots that we had originally identified as relatively high NDVI sites using orbital data were visually dry and dominated with oxidized granite on the surface (Fig. 5) and ultimately proved to have relatively low AFDM and chlorophyll content. Similarly, the hyperspectral data of the field samples measured in the laboratory illustrated clear distinctions between the plots. For example, Plots 20 and 29 were located within oxidized granite boulder fields (according to field notes and photos) and exhibit two broad electronic absorptions associated with the presence of ferrous and ferric iron, centered near 670 nm and 940 nm, and resulting in a broad reflectance peak between these two absorptions at approximately 740 nm (Fig. 6). Hyperspectral reflectance data can clearly distinguish between these abiotic absorption features and those associated with biological pigments; however, multispectral data are less helpful in making this distinction. For this reason, we have shown that the NDVI parameter specifically can be problematic at identifying the presence of photosynthetic biology in the presence of specific abiotic surface properties. This electronic Fe-absorption at red wavelengths and the slight increase in reflectance in the NIR causes these granite areas to have an anomalously high NDVI that does not appear to be correlated with any biological activity.

It is noteworthy that Plot 09 contained a relatively dense community of biocrust (Fig. 1b) and supported a diverse soil food web (*i.e.*, all 3 nematode species were identified here, and tardigrades, rotifers, and ciliates) (Table 1). This area is completely disconnected from streams, is at a higher elevation away from the lake, and appears to only receive moisture from uphill melting snowpacks. While diverse soil food webs are common near the lake and streams of the Ross till, it is impressive that an upland snowpack melt area can sustain a relatively dense community of biocrust supporting a diverse soil food web. Indeed, Plot 09, the only plot with visibly dense biocrust in our field campaign, was visually unique with the highest NDVI in the hyperspectral measurements (*e.g.*, Fig. 6); however, it did not have the highest satellite-derived NDVI as expected. This demonstrates the differences in resolution and capability between a hyperspectral imaging spectrometer and a multispectral satellite. Additionally, this difference could also partly be the result of fluctuating activity, as a January 2019 WorldView image shows higher NDVI at this location when the snow is melting. Therefore, it is apparent that there are factors here, other than photosynthetic biomass, driving NDVI, since Plot 09 did not have the highest satellite-derived NDVI compared to all other plots in this study.

The principal component analyses also indicate that biological activity is not the only factor driving NDVI in this region. There is not a clear pattern between plot types (biocrust, bare soil, versus oxidized granite) in the PCA ordination space that contains the soil environment variables (Fig. 7). Though, we would expect the most habitable plots to be in the direction of increasing NH_4^+ and gravimetric water content vectors, which Plot 09 does follow that trend. The soil environments of the oxidized granite plots do not appear similar based on their inconsistent pattern in ordination space, however. In the PCA of the 8 WV-2 spectral bands and vegetation indices, there is a clear pattern between the plot types (Fig. 8), with the oxidized granite clustering in the top right corner of the ordination space with increasing vegetation index values, and a visual gradient of plots ranging from bare soil to relatively dense biocrust on the opposite side of the ordination. There is separability between the biotic and abiotic surfaces with a detection threshold between ~ 5 and 28 mg/cm^2 AFDM, based on the AFDM values from the two highest biomass plots. It is evident through our analyses that geology in this environment can drive higher NDVI, which is non-indicative of biological activity in this instance, and are instead spectrally dominant areas. However, our hyperspectral data show that these biocrust areas are identifiable and distinct from oxidized granite surfaces.

The Ross till region is geologically variable, and it is now evident that certain geological surface minerals can indicate relatively high NDVI, adding unexpected complexity to our objective of detecting cryptic biological activity. Although satellite imagery can be challenged by these false biological detections from abiotic sources using vegetation indices, we have shown that spectral linear unmixing models are an accurate alternative to detecting low density biocrusts. Using similar methods presented in Salvatore et al. 2021, we are currently applying spectral linear unmixing models to WV-2 and WV-3 orbital data using spectral endmembers collected from our previous field campaign using a hyperspectral imaging spectrometer, including the new oxidized granite endmember from this work. Rather than relying on vegetation indices, we are now applying methods, which were confirmed accurate in the laboratory, to a more complex field environment with varying lithological surface composition.

We have shown that low density biocrusts are indeed found throughout the Ross till region in uplands areas away from streams and have the capacity to support diverse soil food webs. Although geological surface composition can impede accurate use of NDVI on soils, spectral linear unmixing methods are a practical alternative for successful biocrust detection. Given the spatial extent of the terrestrial landscape in the McMurdo Dry Valleys, we anticipate a significant amount of carbon is present in these low density biocrust areas. This work brings us closer in our efforts to refine the carbon budget for this region and to examine the controls over the distribution and activity of these critical soil communities. These remote sensing technologies are ideal for measuring ecosystem dynamics in Antarctic ecosystems which are particularly climate-sensitive and difficult to access.

Acknowledgments

This project was supported by the Virginia Space Grant Consortium 2020 and 2021 Fellowship Programs and the National Science Foundation through Grant #1637708 to the McMurdo Dry Valleys Long Term Ecological Research Project and Grant #1745053 to Salvatore, Barrett, Sokol, and Stanish. We acknowledge the Polar Geospatial Center for geospatial support and DigitalGlobe, Inc. for access to satellite imagery. We appreciate Antarctic Support Contractors and Air Center Helicopters for providing operational support in the field. We would also like to thank Ernest Osburn for assistance with ground truthing and sample collection in the field, and Bobbie Niederlehner, Byron Adams, and Maxwell Craddock for their assistance with laboratory analyses.

References

Adams BJ, Bardgett RD, Ayres E, Wall DH, Aislabie J, Bamforth S, Bargagli R, Cary C, Cavacini P, Connell L, Convey P, Fell JW, Frati F, Hogg ID, Newsham KK, O'Donnell A, Russell N, Seppelt RD, Stevens MI (2006) Diversity and distribution of Victoria Land biota. Soil Biol Biochem 38:3003–3018 . https://doi.org/10.1016/J.SOILBIO.2006.04.030

Alger AS, McKnight DM, Spalding SA, Tate CM, Shupe GH, Welch KA, Edwards R, Andrews ED, House HR (1997) Ecological Processes in a Cold Desert Ecosystem: The Abundance and Species Distribution of Algal Mats in Glacial Meltwater Streams in Taylor Valley, Antarctica. Inst Arct Alp Res Occas Pap 51

Barrett JE, Virginia RA, Hopkins DW, Aislabie J, Bargagli R, Bockheim JG, Campbell IB, Lyons WB, Moorhead DL, Nkem JN, Sletten RS, Steltzer H, Wall DH, Wallenstein MD (2006a) Terrestrial ecosystem processes of Victoria Land, Antarctica. Soil Biol Biochem 38:3019–3034 . https://doi.org/10.1016/J.SOILBIO.2006.04.041

Barrett JE, Virginia RA, Wall DH, Cary SC, Adams BJ, Hacker AL, Aislabie JM (2006b) Co-variation in soil biodiversity and biogeochemistry in northern and southern Victoria Land, Antarctica. Antarct Sci 18:535 . https://doi.org/10.1017/S0954102006000587

Barrett JE, Virginia RA, Wall DH, Parsons AN, Burkins MB (2004) Variation in Biogeochemistry and Soil Biodiversity across Spatial Scales in a Polar Desert Ecosystem. Ecology 85:3105–3118

Bockheim JG, Prentice ML, McLeod M (2008) Distribution of glacial deposits, soils, and permafrost in Taylor Valley, Antarctica. Arctic, Antarct Alp Res 40:279–286 . https://doi.org/10.1657/1523-0430(06-057)[BOCKHEIM]2.0.CO;2

Brenowitz S, Castenholz RW (1997) Long-term effects of UV and visible irradiance on natural populations of a scytonemin-containing cyanobacterium (Calothrix sp.). FEMS Microbiol Ecol 24:343–352 . https://doi.org/10.1016/S0168-6496(97)00075-5

Couradeau E, Karaoz U, Lim HC, Nunes Da Rocha U, Northen T, Brodie E, Garcia-Pichel F (2016) Bacteria increase arid-land soil surface temperature through the production of sunscreens. Nat Commun. https://doi.org/10.1038/ncomms10373

Courtright EM, Wall DH, Virginia RA (2001) Determining habitat suitability for soil invertebrates in an extreme environment: The McMurdo Dry Valleys, Antarctica. Antarct Sci 13:9–17 . https://doi.org/10.1017/S0954102001000037

Doran PT, McKay CP, Clow GD, Dana GL, Fountain AG, Nylen T, Lyons WB (2002) Valley floor climate observations from the McMurdo dry valleys, Antarctica, 1986–2000. J Geophys Res 107:4772 . https://doi.org/10.1029/2001JD002045

Fountain AG, Fernandez-Diaz JC, Obryk M, Levy J, Gooseff M, Van Horn DJ, Morin P, Shrestha R (2017) High-resolution elevation mapping of the McMurdo Dry Valleys, Antarctica, and surrounding regions. Earth Syst Sci Data 9:435–443 . https://doi.org/10.5194/essd-9-435-2017

Freckman DW, Virginia RA (1997) Low-diversity antarctic soil nematode communities: Distribution and response to disturbance. Ecology 78:363–369 . https://doi.org/10.1890/0012-9658(1997)078[0363:LDASNC]2.0.CO;2

Freckman DW, Virginia RA (1993) Extraction of nematodes from Dry Valley Antarctic soils. Polar Biol 13:483–487 . https://doi.org/10.1007/BF00233139

Garcia-Pichel F, Castenholz RW (1991) Characterization and Biological Implications of Scytonemin, a Cyanobacterial Sheath Pigment. J Phycol 27:395–409 . https://doi.org/10.1111/j.0022-3646.1991.00395.x

Levy J (2013) How big are the McMurdo Dry Valleys? Estimating ice-free area using Landsat image data. Antarct Sci 25:119–120 . https://doi.org/10.1017/S0954102012000727

Marchant DR, Denton GH (1996) Miocene and Pliocene paleoclimate of the Dry Valleys region, Southern Victoria land: A geomorphological approach. Mar Micropaleontol 27:253–271 . https://doi.org/10.1016/0377-8398(95)00065-8

McKnight DM, Niyogi DK, Alger AS, Bomblies A, Conovitz PA, Tate CM (1999) Dry Valley Streams in Antarctica: Ecosystems Waiting for Water. Bioscience 49:985–995 . https://doi.org/10.1525/bisi.1999.49.12.985

Pannewitz S, Green TGA, Scheidegger C, Schlensog M, Schroeter B (2003) Activity pattern of the moss Hennediella heimii (Hedw.) Zand. in the Dry Valleys, Southern Victoria Land, Antarctica during the mid-austral summer. Polar Biol 26:545–551 . https://doi.org/10.1007/s00300-003-0518-8

Poage MA, Barrett JE, Virginia RA, Wall DH (2008) The influence of soil geochemistry on nematode distribution, Mcmurdo Dry Valleys, Antarctica. Arctic, Antarct Alp Res 40:119–128 . https://doi.org/10.1657/1523-0430(06-051)[POAGE]2.0.CO;2

Power SN, Salvatore MR, Sokol ER, Stanish LF, Barrett JE (2020) Estimating microbial mat biomass in the McMurdo Dry Valleys, Antarctica using satellite imagery and ground surveys. Polar Biol 43:1753–1767 . https://doi.org/10.1007/s00300-020-02742-y

Salvatore MR (2015) High-resolution compositional remote sensing of the Transantarctic Mountains: application to the WorldView-2 dataset. Antarct Sci 27:473–491 . https://doi.org/10.1017/S095410201500019X

Salvatore MR, Barrett JE, Borges SR, Power SN, Stanish LF, Sokol ER, Gooseff MN (2021) Counting Carbon: Quantifying Biomass in the McMurdo Dry Valleys through Orbital & Field Observations. Int J Remote Sens 42:8597–8623 . https://doi.org/10.1080/01431161.2021.1981559

Salvatore MR, Borges SR, Barrett JE, Sokol ER, Stanish LF, Power SN, Morin P (2020) Remote characterization of photosynthetic communities in the Fryxell basin of Taylor Valley, Antarctica. Antarct Sci 1–16 . https://doi.org/10.1017/S0954102020000176

Schwarz AMJ, Green TGA, Seppelt RD (1992) Terrestrial vegetation at Canada Glacier, Southern Victoria Land, Antarctica. Polar Biol 12:397–404 . https://doi.org/10.1007/BF00243110

Thrane J-E, Kyle M, Striebel M, Haande S, Grung M, Rohrlack T, Andersen T (2015) Spectrophotometric Analysis of Pigments: A Critical Assessment of a High-Throughput Method for Analysis of Algal Pigment Mixtures by Spectral Deconvolution. PLoS One 10:e0137645 . https://doi.org/10.1371/journal.pone.0137645

Treonis A, Wall D, Virginia R (1999) Invertebrate biodiversity in Antarctic Dry Valley soils and sediments. Ecosystems 2:482–492

Tucker CJ (1979) Red and Photographic Infrared Linear Combinations for Monitoring Vegetation. Remote Sens Environ 8:127–150

Young KE, Reed SC (2017) Spectrally monitoring the response of the biocrust moss Syntrichia caninervis to altered precipitation regimes. Sci Rep 7:1–10 . https://doi.org/10.1038/srep41793